Ion velocity distributions in front of a ceramic surface: an inverse sheath ?

V. Pigeon[1], N. Claire[1], C. Arnas[1]

[1] *Aix-Marseille University, CNRS, PIIM, Marseille, France*

Abstract

It is shown that there is no inverse sheath in front of insulator ceramic sample ($BNSiO_2$, Hall thruster's relevant material) immersed in a hot cathode discharge plasma. Laser optical pumping saturation induces laser induced fluorescence (LIF) measurements artifacts, which are evolving along the pre-sheath and the sheath. Therefore, the determination of the right ion velocity distribution function has to be carefully performed when LIF measurements are made close to a surface reflecting the laser beam. Nevertheless, the $BNSiO_2$ sheath and pre-sheath width is unexpectedly large, several centimeters, as the wall ion velocity, $\sim$ 18 km/s, compared to a metallic surface and theoretical model results.

The experiments are performed in a multipolar plasma device [1, 2], see Fig. 1. The discharge is created by two Tungsten filaments, negatively biased to 100 V with respect to the grounded vacuum vessel. The heating current is monitored in order to maintain a stable discharge current of 0.5 A. The working pressure is 10^{-4} mbar. The Argon plasma has the following parameters: density $n = 10^{15}$ m^{-3}, electronic plasma temperature of $T_e = 1.5$ eV, ionizing electron temperature of $T_{ep} = 12$ eV. The Debye length is $\lambda_D \sim 0.3mm$ and the plasma potential is $\phi_p = 5$V.

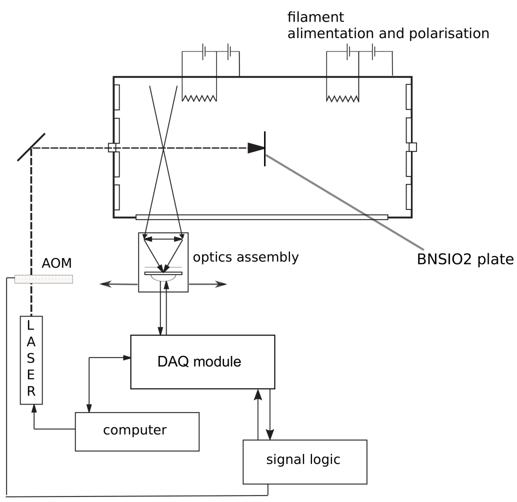

Figure 1: *Sketch of the multipolar device with the acquisition system.*

The LIF is used in plasmas for decades [3, 4, 5]. This diagnostic relies on the excitation of a wisely chosen electronic transition of an ion (or atom) and the Doppler effect. Using a frequency tunable laser it is possible to combine these effects to measure ionic (or atomic) velocity distribution function (IVDF) along the laser beam, thanks to the detection of the induced fluorescence photons. Generally ions are excited from a level 1, usually a metastable one in order to have a sufficient lifetime to represent ions behavior, to a short lifetime level 2. The fluorescence signal corresponds to the fast deexcitation photon from the level 2 to a third level. The main advantages

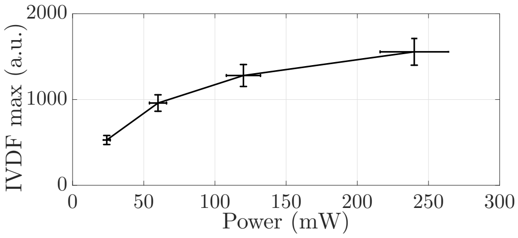

Figure 2: *IVDF maximum with respect to the laser beam power.*

of this technique are its non-invasive nature and its good spatial and temporal resolution, which are relevant to study plasma sheaths that are in most cases thin and easily perturbed [1, 2].

Performing LIF in a sheath implies that a surface is present and reflects the laser beam, which may cause some undesired additional signal. This can be avoided by drilling a hole in the surface or using a beam bumper to cancel out the reflection [6, 7, 8]. Also, the experimental set-up has to provide a resolution high enough to probe this plasma region, where the potentiel gradient is important, and so the spatial gradient of the IVDF [1].

Optical pumping saturation effect is one of the possible experimental bias of the diagnostic. It occurs when the laser beam pumping rate from level 1 to level 2 is about the order of magnitude of (or larger than) the creation rate of level 1 by inelastic electron-ion collisions in the plasma [9, 10, 11]. When this happens, the signal intensity is no more proportional to power density and the IVDF is broadened.

Saturation does occur in the present experiment. Fig. 2 shows the LIF maximum signal level as a function of the laser power in the bulk plasma, where the IVDF is a maxellian distribution at rest. This curve suggests that saturation effects begin around 50 mW in our plasma since the fluorescence signal is no more proportional to the laser power. Unfortunately, our diagnostic does not allow measurements with higher or lower power.

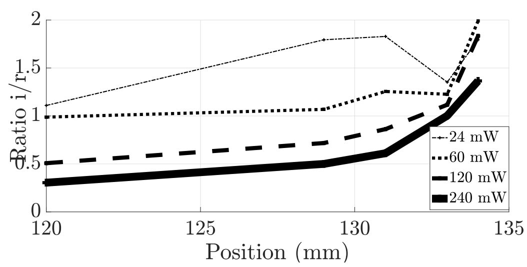

Figure 3: *Ratio between incident and reflected beam peaks maxima in front of the BNSi02 ceramic. The sample is located at 136mm.*

This LIF signal saturation influences the global signal shape. Fig. 3 shows the IVDF maximum level ratio between the signal corresponding to the incident beam and the one reflected by the BNSiO2 surface with respect to the wall distance. It appears that for high laser power, the reflected beam signal intensity is larger than the incident one. Since the power density of the reflected beam is much lower than the incident beam one, the first may not saturate the LIF transition while the second does. Also, the measurement volume of the first one is larger than the second one (the signal is collected along a cone). Before its identification, this experimental could has bias led to a wrong interpretation of the data: the inverse sheath hypothesis.

The ratio also evolves along the sheath and the pre-sheath, as well as the density of the distribution function. Fig. 4 shows the metastable density with respect to the wall distance. The increase of the density in the presheath, which was previously measured for a conducting wall[1], is also related to saturation effects. The density drop in the vicinity of the surface induces stronger LIF signal saturation and is characterized by a broadening of the distribution function which does not ensure accurate density measurements.

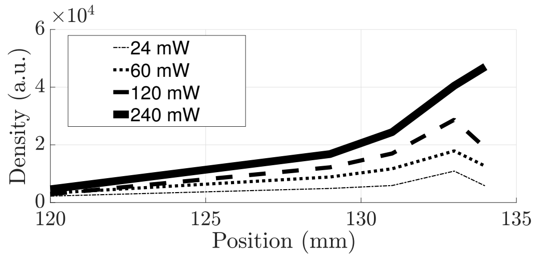

Figure 4: *Density in front of the ceramic plate, for several laser powers. Ceramic is located at* 136 *mm*

Experimental artifacts have been identified, which allowed the sheath characterization. Fig. 5 shows the metastable ion fluid velocity v as a function of wall distance with a laser power of 15 mW. This first measurement of IVDF in an insulator ceramic's sheath shows a large wall ion velocity $\sim$ 18km/s. The pre-sheath extends far from the surface, up to 3 cm. Considering collisionless sheath/pre-sheath, fluid energy conservation may be used for sheath potential ϕ calculation: $\frac{1}{2}m_i v^2 = -e(\phi - \phi_p)$. The $BNSiO_2$ floating potential is $\phi_{f_c} = -66$ V, which is much lower than the floating potential of a tungsten Langmuir probe $\phi_{f_p} = -35$ V with identical experimental conditions. Also, the floating potential calculated with a theoretical model [12], including the hot electron population and realistic secondary electron emission from the wall [13], gives a floating potential close to -35V. This large discrepancy, which was observed for various plasma parameters, is currently under investigation.

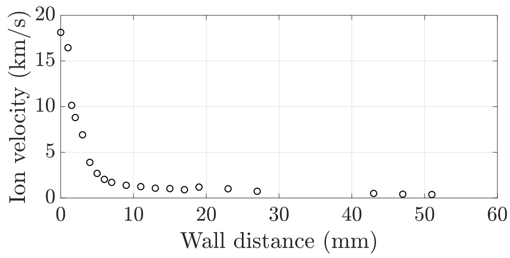

Figure 5: *Ion fluid velocity with respect to the wall distance.*

Conclusion

The choice of the incident beam signal for LIF diagnostic must be carefully made when a surface is present, since LIF transition saturation may lead an inverted ratio between the incident beam and reflected beam signals. Moreover, this optical pumping saturation evolves along the presheath and the sheath, suggesting that variations of the metastable density exist in these regions.

These first measurements of IVDFs in the sheath of an insulator material, $BNSiO_2$, show that a long presheath exists, the ion velocity close to the surface is large, and the surface potential is lower than a metallic floating one. Secondary electron emission, which is higher for this material than for metals, could not be enough to explain this difference, as shown by the theoretical model prediction [12]. The difference between the Langmuir probe floating potential and the the ceramic one suggests that other phenomena occur for insulator material. These features, specific to an insulator material still need to be identified. A comparison between several insulators (ceramics and glass), metals and semi-conductors (silicon) is currently performed to highlight such effects in different plasma reactors, with our without ionizing electrons responsible of secondary electron emission.

References

[1] N. Claire, G. Bachet, U. Stroth and F. Doveil, Physics of Plasmas **13**, 062103 (2006)

[2] N. Claire, S. Mazouffre, C. Rebont and F. Doveil, Physics of Plasmas **19**, 032108 (2012)

[3] R. M. Measures, Journal of Applied Physics **34**, 1548–1551 (1975)

[4] R. A. Stern and J. A. Johnson, Physical Review Letters **39**, 5232–5245 (1968)

[5] D.N. Hill, S. Fornaca and M. G. Wickham, Review of Scientific Instruments **54**, 309–314 (1983)

[6] T. Lunt, G. Fussmann and Ole Waldmann, Physical Review Letters **100**, (2008)

[7] D. Lee, G. Severn, L.O. and Noah Hershkowitz, Journal of Physics D: Applied Physics **24**, 5230–5235 (2006)

[8] C.S. Yip, N. Hershkowitz and G. Severn, Physical Review Letters **104**, (2010)

[9] R. Altkorn, R.N. Zare, N. Hershkowitz and G. Severn, Annual Review of Physical Chemistry **35**, 265–289 (1984)

[10] M. J. Goeckner, J. Goree and T. E. Sheridan, Review of Scientific Instruments **64**, 996–1000 (1993)

[11] F. Chu and F. Skiff, Physics of Plasmas **25**, 013506 (2018)

[12] Langendorf, S. and Walker, M., Physics of Plasmas **22**, 033515 (2015)

[13] T. Tondu, M. Belhaj, V. Inguimbert, Journal of Applied Physics., **110**, 093301 (2011)